Analysis of the Dependence of the Viewing Zones on the Display Radius in Autostereoscopic 2 View Displays of Horizontally Concave Surface

Hyung Ki Hong

***Abstract*—In autostereoscopic display, ray trajectories through the optic element such as the parallax barrier or the lenticular lens are affected by the radius of horizontally concave display. Using the intersection of the calculated trajectories of the rays coming from the various positions of the autostereoscopic 2 view display of the curved surface, the viewing zones and area of the incomplete separation of the images for the left and right eyes were investigated. The area of incomplete separation of the images for the left and right eyes related to the triangular areas defined by three chief rays coming from the left edge, center, and the right edge. These triangular areas for the curved surface was smaller than those for the flat surface and showed the tendency of the decrease as the ratio of the radius of the curved and the designed viewing distance approached 1/2.**

***Index Terms*—Three-dimensional displays.**

I. Introduction

THE research for the flexible display were recently gaining much attention [1]–[5]. And the possible merit of the curved displays and the radius for the best performance were reported as well [6]–[8]. Design principle of autostereoscopic 3D displays which did not need any special eyeglasses to perceive 3D depth, had been well known for the display of the flat surface [9]–[14]. Curved displays having the finite radius along the horizontal direction, had been recently commercialized for TV and the mobile application.

As the curved display became more popular, autostereoscopic 3D using the curved surface needed to be considered. Design principle of autostereoscopic 3D with the curved surface was recently reported [15]. The ray trajectories inside autostereoscopic display are different for the flat and the curved surface. Hence, the optical characteristic of the curved autostereoscopic display may be affected by the radius of the curved display.

In this paper, the optical characteristics of autostereoscopic 2 view display using the parallax barrier were compared for the horizontally concave surface of the various radii. Among the various optical characteristics, the investigation of this paper focused on the positions of the viewing zones and the area of the good image separation for the left and right eyes at the curved surface of the various radii. For this purpose, the trajectories of the rays coming from the left edge, the center and the right edge of the autostereoscopic display through the aperture of the parallax barrier were calculated for the various ratios between the display radius and the designed viewing distance. From the spatial distribution of the trajectories of the rays coming from the pixel boundaries and the active area of each pixel of the autostereoscopic displays, the viewing zones and the separation of images for the left and right eyes were investigated.

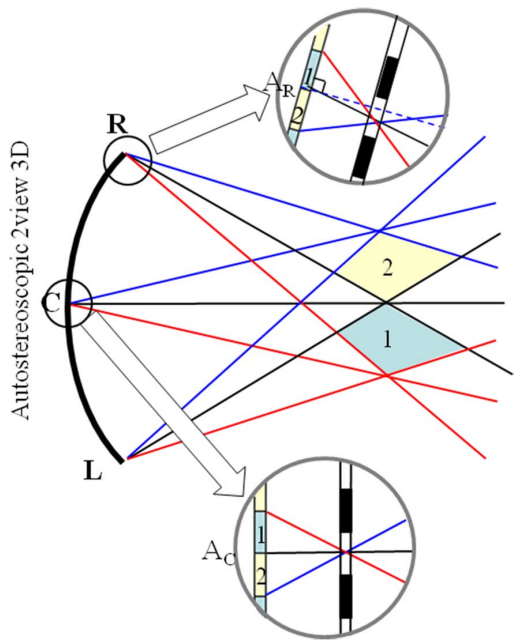

Fig. 1. Intersections of three rays from the corresponding pixel boundary at the left edge L, the center C, and the right edge R determine the viewing zone of autostereoscopic 2 view display.

II. Background

The viewing zones of autostereoscopic displays were determined by the light rays coming from the various positions of the display. For the optical design principle of the autostereoscopic display, the boundaries of the viewing zone of autostereoscopic display had been defined by three rays coming from the corresponding positions on the right edge, center and left edge of the display. Fig. 1 illustrates the concept of autostereoscopic display

Manuscript received October 01, 2015; revised January 14, 2016; accepted February 29, 2016. Date of publication March 16, 2016; date of current version June 30, 2016. This work was supported by the Research Program funded by the Seoul National University of Science and Technology.

The author is with Seoul National University of Science and Technology, Seoul 139-743, Korea (e-mail: hyungki.hong@snut.ac.kr).

Color versions of one or more of the figures in this paper are available online at http://ieeexplore.ieee.org.

Digital Object Identifier 10.1109/JDT.2016.2542826

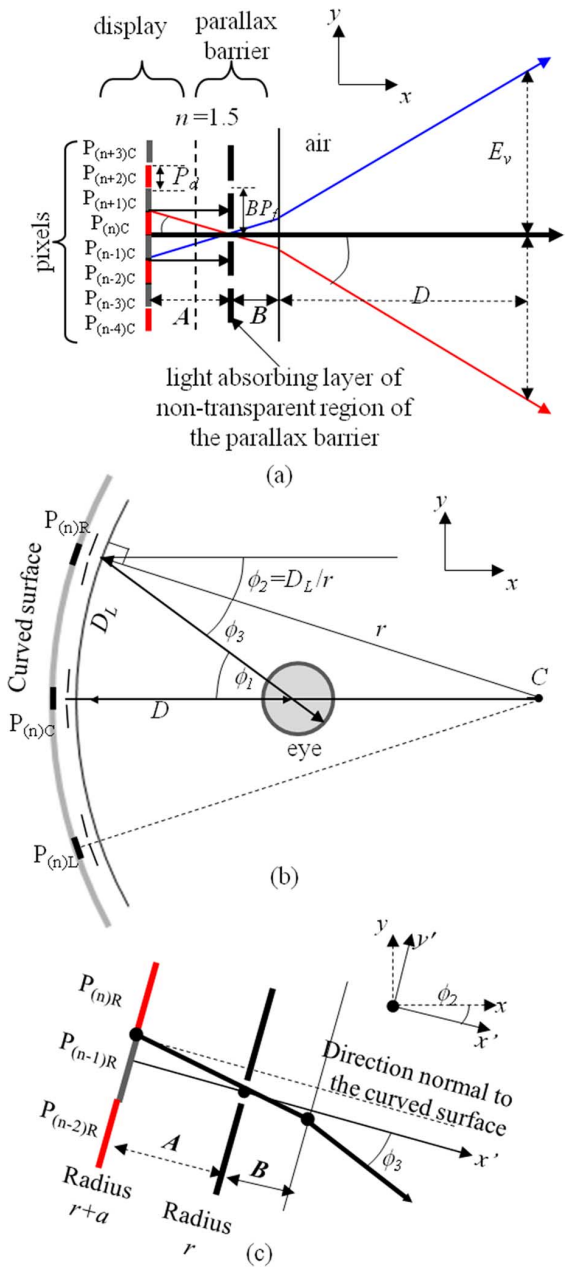

Fig. 2. Simulation scheme (a) Configuration at the center of the display (b) The relation between radius R and angles (c) Configuration at the right edge of the display. Curved display with the horizontally concave surface and the radius of R was considered. Rays come out from the pixel boundaries of the autostereoscopic display.

using the curved surface and the parallax barrier. Design principle for FPD had been well known [12]–[14]. And recently the optical design principle for curved display had been reported for 2view display using the parallax barrier. [15]

In the example of Fig. 1, the position A_C was located at the boundaries of the two pixels for view 1 and view 2 at the center of the display. And the line passing through A_C and the center of the transparent region of the parallax barrier was selected to be normal to the surface at the center of the display.

In case of the position A_R located at the boundaries of the two pixels for view 1 and view 2 at the right edge of the display, the

TABLE I
PARAMETERS FOR THE CALCULATION OF AUTOSTEREOSCOPIC 2 VIEW AT THE DESIGNED VIEWING DISTANCE OF 300 MM

D(mm) : Designed viewing distance			300
angle ϕ1 (deg)			14.85
Pd(μm): Pixel size			81
Horizontal pixel numbers			1920
A(μm): distance between pixel and barrier			570
B(μm): distance between the air and barrier			200
Barrier aperture ratio(%)			15
radius r (mm)	infinite	BPf(mm) Barrier pitch	161.7984
		angle f3(deg)	14.83
	300 (equal to D)	BPf(mm) Barrier pitch	161.6929
		angle f3(deg)	0
	150 (half of D)	BPf(mm) Barrier pitch	161.5937
		angle f3(deg)	-14.85

TABLE II
PARAMETERS FOR THE CALCULATION OF AUTOSTEREOSCOPIC 2 VIEW AT THE DESIGNED VIEWING DISTANCE OF 600 MM

D(mm) : Designed viewing distance			600
angle ϕ1 (deg)			28.42
Pd(μm): Pixel size			155
Horizontal pixel numbers			3840
A(μm): distance between pixel and barrier			2290
B(μm): distance between the air and barrier			200
Barrier aperture ratio (%)			15
radius r (mm)	infinite	BPf(mm) Barrier pitch	309.2625
		angle f3(deg)	28.39
	600 (equal to D)	BPf(mm) Barrier pitch	308.8203
		angle f3(deg)	0
	300 (half of D)	BPf(mm) Barrier pitch	308.4452
		angle f3(deg)	-28.42

direction of the line passing through A_R and the center of the transparent region of the parallax barrier should be shifted toward the eye of the viewer. The amount of the shifted angle was determined by the designed viewing distance and the radius of the curved display. Direction normal to the surface of FPD was always the same while direction normal to the curved surface changes depending on the radius of the curved surface. Therefore, the ray distribution coming from the left and right edges were different between the FPD and the curved display. This difference would affect the optical characteristics of autostereoscopic display.

III. SIMULATION

Configuration of autostereoscopic 2 view display using the parallax barrier was designed for the simulation as illustrated in Fig. 2. Parameters for the calculation of the ray trajectories were shown in Table I and II for the designed viewing distance D of 300 mm and 600 mm. The designed viewing distance D of 300 m for mobile application and 600 for monitor application were considered. Pixel size P_d and the horizontal pixel numbers for these applications were respectively selected. In Fig. 2(a), the trajectories of chief rays from the pixel boundaries through the center of the each aperture of the parallax barrier to the user position were illustrated. E_v, which was the distance between

the adjacent viewing zones, was selected to be 65 mm. The distance ***A*** represents the distance from the pixel to the light absorbing layer of the parallax barrier. The distance ***B*** represents the distance from the light absorbing layer of the parallax barrier to the boundary with the air. Pixels $\mathrm{P}_{(\mathrm{n})\mathrm{c}}$ where n was even or odd number represented the pixels assigned to the two viewing zones, respectively. Due to the parallax barrier, the rays coming from these pixels can be seen only at the specific positions. In Fig. 2(b), Pixels $\mathrm{P}_{(\mathrm{n})\mathrm{R}}$ and $\mathrm{P}_{(\mathrm{n})\mathrm{L}}$ at the right and the left edge of the displays represented the position corresponding to the pixel $\mathrm{P}_{(\mathrm{n})\mathrm{C}}$ at the center of the display. Angle ϕ_1 represented the angle from the edge of the display to the eye of the user and was determined by the designed viewing distance D and the horizontal display size. In curved surface, the normal direction at the edge of the display was shifted by the amount of angle ϕ_2 from the x-axis, due to the curvature of the display.

Angle ϕ_3 represented the angular change caused by the difference between the pixel size and the barrier pitch BP_d. The sum of ϕ_2 and ϕ_3 is equal to ϕ_1. In case of the flat surface, the angle ϕ_2 was zero. If the radius was the same as the viewing distance, the angle ϕ_1 was the same as the angle ϕ_2 and the angle ϕ_3 was zero. Ray trajectories at the edge of the display were calculated in the $x'y'$ coordinate system. In the $x'y'$ coordinate system, the direction of x'-axis was selected to be normal to the display surface and the axes were rotated by the amount of ϕ_2 from the *xy* coordinate system as illustrated in Fig. 2(c).

Ray trajectories were investigated at conditions that the radius r of the concave surface was a half or the same. Ray trajectories for display of the flat surface were also investigated for comparison.

For autostereoscopic two view display, the barrier pitch for flat surface had been reported as [11], [15]

$$BP_p^{flat} = \frac{2}{1/P_d + 1/E_v} \tag{1}$$

In (1), P_d and E_v represent the pixel size and the distance between the adjacent viewing zones.

For autostereoscopic two view display of the curved surface, the barrier pitch BP_d and the distance $\mathbf{A}$ and $\mathbf{B}$ were determined by the reported design scheme [15].

$$BP_p^{curved} = 2P_d\frac{r+B}{r+B+A} - \frac{BS_C}{M} \tag{2}$$

where $BS_c = a\tan(\sin^{-1}(\frac{\sin\phi_3}{n}))$

M was defined as the half of the horizontal pixel numbers. The values of the barrier pitch in Table I and II were derived from (1) in case of the flat surface and from (2) in case of the curved surface. Matlab was used to calculate and visualize the ray trajectories of the configuration of autostereoscopic display of Fig. 2[16].

IV. Result and Discussion

Fig. 3 illustrated the calculated trajectories of the chief rays coming from the corresponding positions of the pixel boundaries on the right edge, center and left edge of the display as illustrated in Fig. 2. The viewing distance D of 300 mm and the display radius r of 300 mm and the parameters of Table I were used for the calculation. The trajectories of 3 chief rays had been

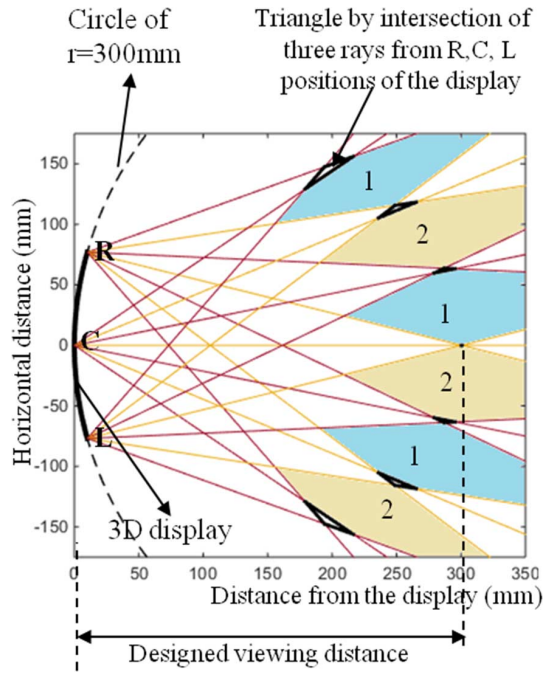

Fig. 3. Calculated trajectories of chief rays coming from the pixel boundaries and the viewing zone at the designed viewing distance D of 300 mm and the display radius r of 300 mm for auto stereoscopic 2 view display. Thick solid line on the left side represents the display of the curved surface. The dotted curve represents the circle with the same radius as the curved display. Horizontal and vertical axes represent the distance from the display surface and horizontal distance from the center of the display. R, C and L represent the right edge, center, left edge of the display, respectively. Shaded area 1 and 2 represent the viewing zones.

used to define the viewing zones of view 1 and 2 [11]–[14]. In the calculated result of Fig. 3, these rays intersected at the one point on the line perpendicular to the center of the display. Yet, these three rays formed the triangles of the finite sizes near the viewing zones for view 1 and 2 at other positions. It showed the trend that the triangle size became larger for the positions of the larger horizontal distance from the center of the display. Intersection of these chief rays at one position meant that the eye located on that position could see the corresponding positions on the autostereoscopic display. The triangular areas could be considered as the areas that the separation of the images for the left and right eyes were incomplete. For example, if the eye was located on the intersection of only two chief rays coming from the pixel boundaries of the left and right edge of the display for the finite triangle size, the eye would not see the pixel boundaries at the center of the display. Hence, the size of the triangle could be used as the indicator that the smaller size of these triangles implies the better separation between the adjacent viewing zones.

Fig. 4(a) illustrated the calculated trajectories of the 3 chief rays with the same calculation conditions as Fig. 3 except that the curved surface of the radius of 150 mm and the flat surface was used. The calculated sizes of triangles by three chief rays were different for the different radius. In Fig. 4(b), these triangles calculated for the different radius at the designed viewing distance of 300 mm were shown together for the easier comparison. For the smaller radius, the triangle size tended to decrease. When the radius r was 150 mm which was a half of the viewing

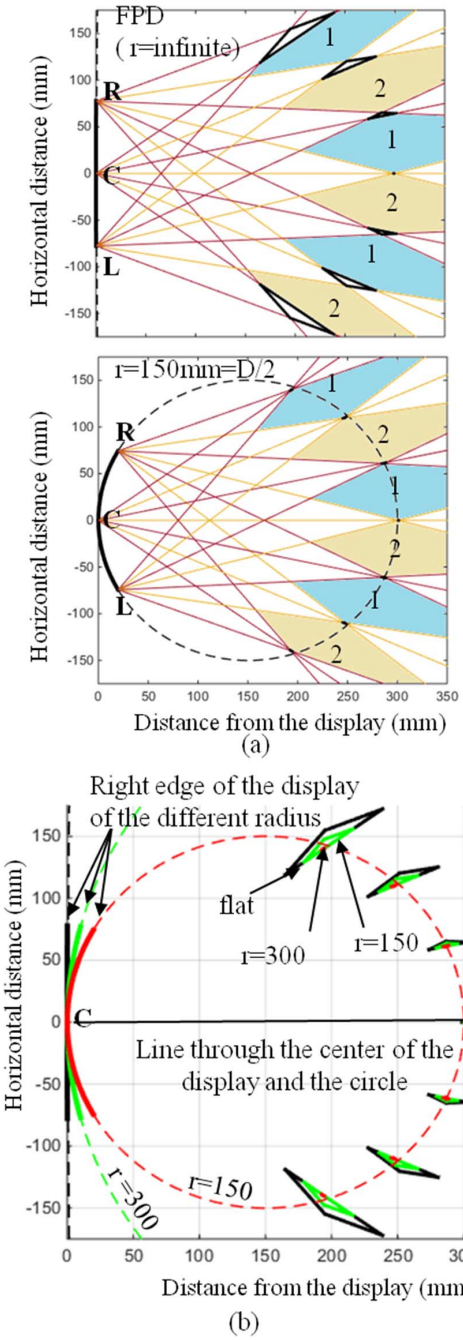

Fig. 4. Result at the designed viewing distance D of 300 mm. (a) Calculated trajectories of chief rays coming from the pixel boundaries and the viewing zone at the radius r of 150 mm and the flat surface for autostereoscopic 2view display. Shaded area 1 and 2 represent the viewing zones. (b) Triangles by the intersection of the calculated trajectories of 3 chief rays coming from the pixel boundaries at the center, the left edge and the right edge of the display for the various radius of the curved display for autostereoscopic 2view display. Notations in the graph are the same as those of Fig. 3.

distance D, triangles were almost located on the same circle as the display surface and the triangle size remained quite small irrespective of horizontal distance.

In Fig. 3 and 4(a), the shapes and the position of the viewing zones were similar for the three different radii [11]. The distance to the position of the viewing zones was approximately equal to the designed viewing distance, only near the center of the display. That the distance to the positions of the viewing zones was not constant, had been reported, though the shape of the positions of the viewing zones was not described [14]. Fig. 3 and 4 showed that the positions of the viewing zones could be approximated by the circle whose radius was a half of the viewing distance.

Fig. 5 illustrated the calculated result for the viewing distance D of 600 mm. Parameters for the calculations were on Table II. The radius of the curved display was selected to be 300 mm and 600 mm. Trajectories for the flat surface were also calculated. Similar to the case of the viewing distance D of 300 mm, the triangle sizes became smaller for the smaller r as illustrated in Fig. 5(b).

As the trajectories of the chief rays from the three positions on the displays showed the positions of the viewing zones only for the ideal, other conditions were investigated for the practical situation.

In Fig. 4 and 5, trajectories of chief rays from only 3 positions were calculated while in practical situation, rays from other positions on the display needed to be considered. Fig. 6 illustrated the calculated result for the viewing distance D of 600 mm for the flat surface and the curved surface of the radius of 300 mm where 9 chief rays coming from the display were considered. Around the designed viewing distance, trajectories of these 9 rays roughly converged to the triangles area by the intersection of the calculated trajectories of chief rays from the center, the left edge and the right edge of the display. Hence, 3 chief rays from the center, the left edge and the right edge could be considered to be enough to represent the characteristics of rays coming from the other positions on the display.

For each position on the display, rays other than chief ray also came through the parallax barrier unless the aperture at the parallax barrier was infinitesimal. For the practical situation, the barrier aperture ratio of 15% was assumed and trajectories of multiple rays through the aperture were calculated as illustrated in Fig. 7. Fig. 7(a) illustrates the multiple rays including the chief ray passing through the aperture of the parallax barrier. Fig. 7(b) illustrated the trajectories from the left edge, the center and the right edge of the display for the designed viewing distance D of 600 mm. The rays diverged near the designed viewing distance and the barrier aperture ratio would affect the divergence of these rays. As these diverging rays from one position on the display gathered around each chief ray, trajectories of these rays also formed the rough triangular shape around the triangles by three 3 chief ray. So, in practical situation including rays other than the chief rays, the boundaries of the viewing zone could not be sharply defined. As triangular area by these diverging multiple rays could not be smaller than triangles by three 3 chief ray, the size of the triangles by 3 chief rays would be still useful as the indicator to represent the areas that the separation of the images for the left and right eyes were incomplete.

The calculated result of Fig. 3–7 showed the trajectories of rays from the pixel boundaries and the intersections of these rays related to the boundaries of the viewing zone. In case of autostereoscopic display using the displays of the fixed pixel size such as LCD or OLELD, little light came out from these pixel boundaries which were general called Black Matrix (BM). The area that light actually came out in each pixel was called the active area and located outside the BM. The trajectories of rays

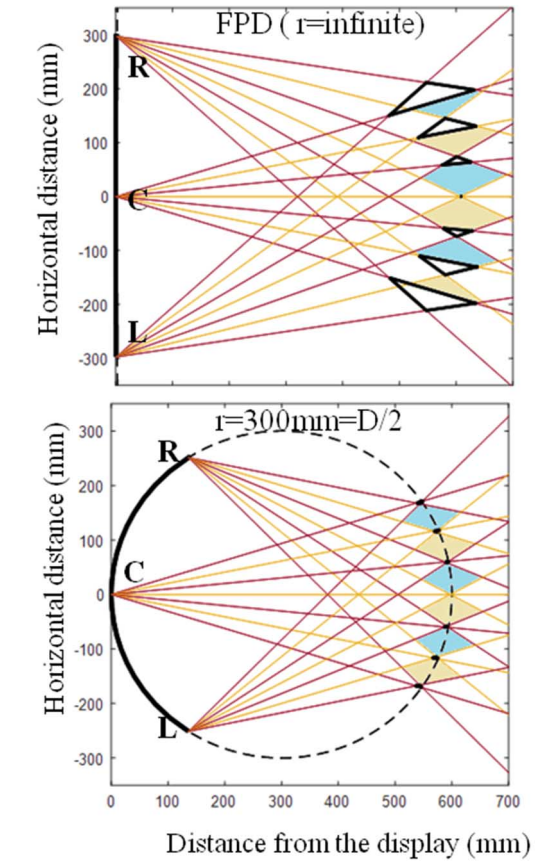

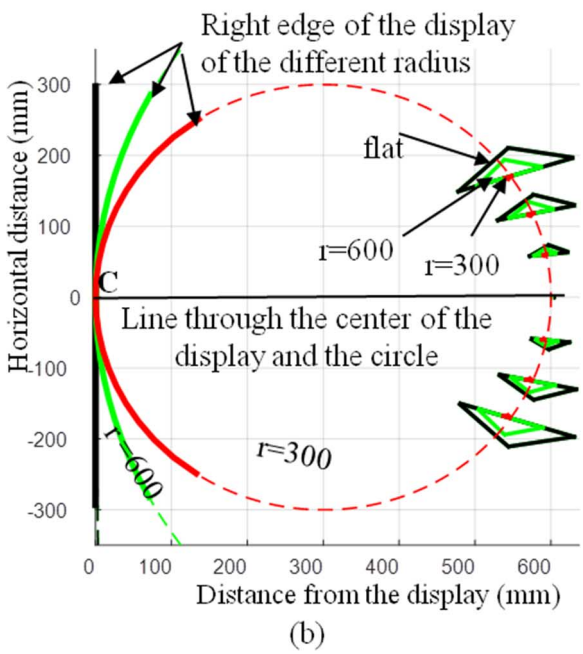

Fig. 5. Result at the designed viewing distance D of 600 mm (a) calculated trajectories of chief rays coming from the pixel boundaries and the viewing zone at the radius r of 300 mm and the flat surface for autostereoscopic 2view display. Shaded area 1 and 2 represent the viewing zones. (b) Triangles by the intersection of the calculated trajectories of 3 chief rays coming from the pixel boundaries at the center, the left edge and the right edge of the display for the various radius of the curved display for autostereoscopic 2view display. Notations in the graph are the same as those of Fig. 3.

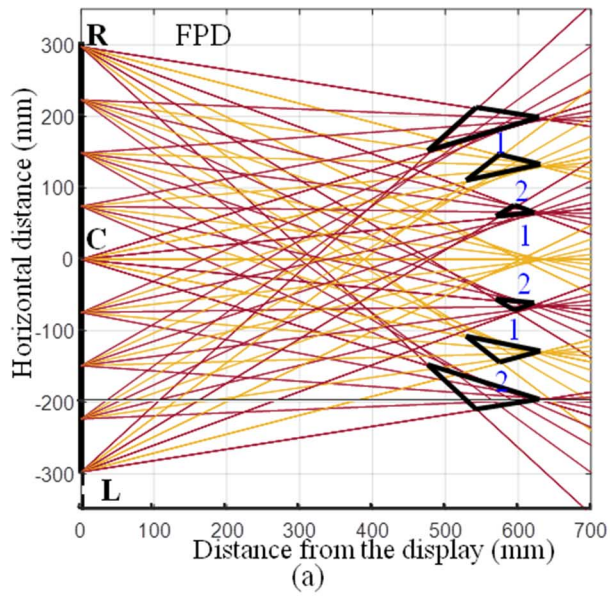

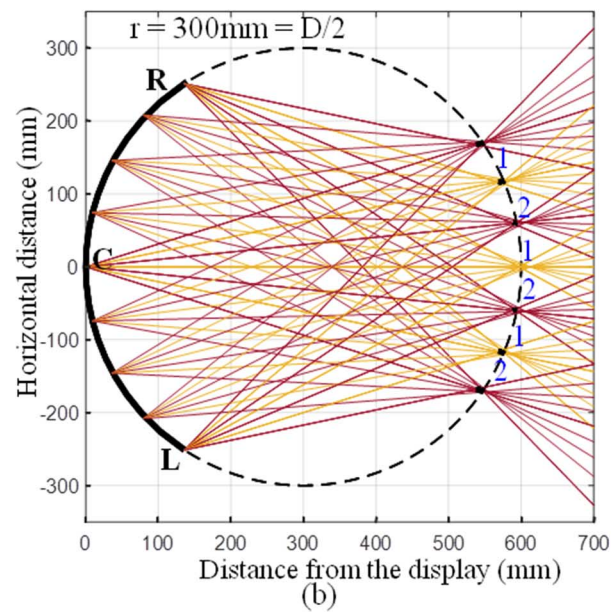

Fig. 6. Calculated trajectories of chief rays coming from the pixel boundaries from 9 position of the 3D display at the designed viewing distance D of 600 mm for (a) the flat surface and (b) the curved surface of r = 300 mm. Triangles represent the intersection of the calculated trajectories of chief rays from the center, the left edge and the right edge of the display.

coming out from 5 positions in the active area of each pixel were calculated as illustrated in Fig. 8(a). Among 5 positions in active area of each pixel, 2 positions were selected to be located at the boundaries of BM and the active area of each pixel. The width of BM was selected to be 20% of the pixel size and the barrier aperture ratio of 15% was selected.

In autostereoscopic display, pixel should be seen by only one of two eyes. The rays coming from the active area of these two kinds of pixels were represented as lines of different colors. And the calculated trajectories were illustrated in Fig. 8(b) for the viewing distance of 600 mm at the autostereoscopic display of the flat and the curved surface. Around the viewing distance, areas that lines of only one colors were located represented the position that each eye could see only the pixels assigned for

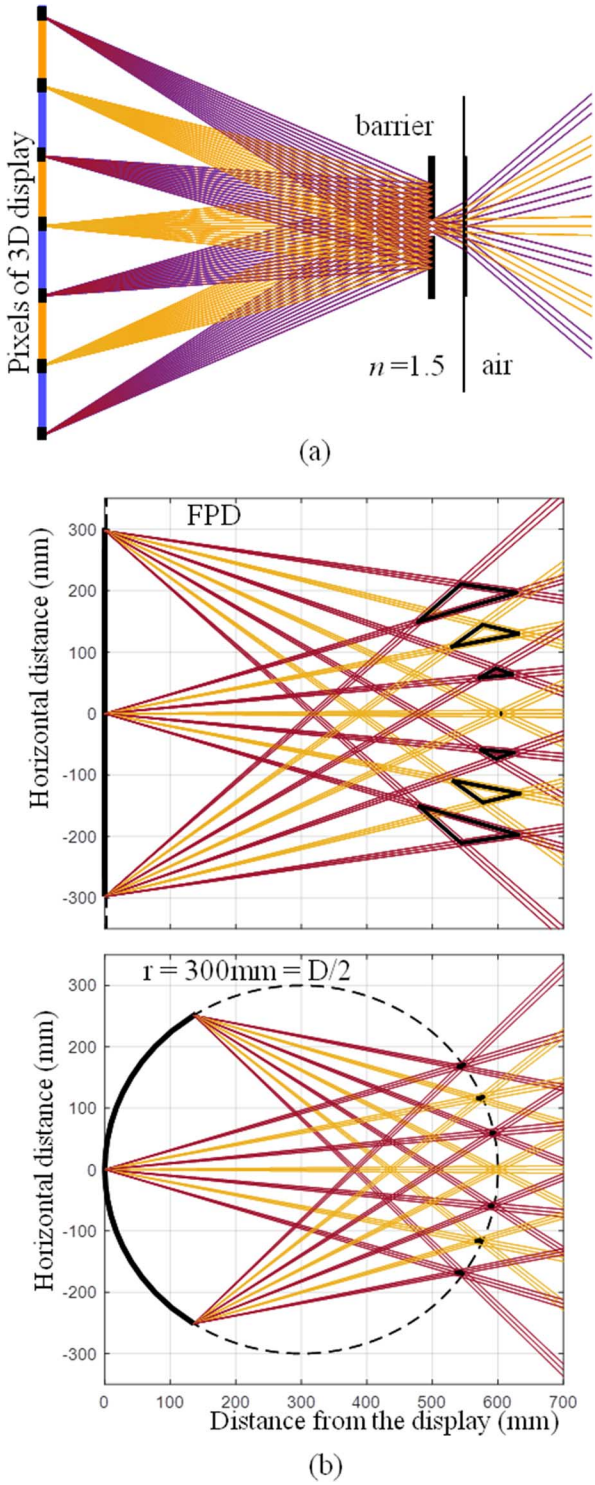

Fig. 7. (a) Trajectories of multiple rays coming from the pixel boundaries of the autostereoscopic display through the parallax barrier. (b) Calculated trajectories of multiple rays from the pixels boundaries at the three positions on the display for the viewing distance D of 600 mm for the flat surface and curved surface of radius r of 300 mm. Barrier aperture ratio was 15%. Triangles represent the intersection of the calculated trajectories of chief rays from the center, the left edge and the right edge of the display.

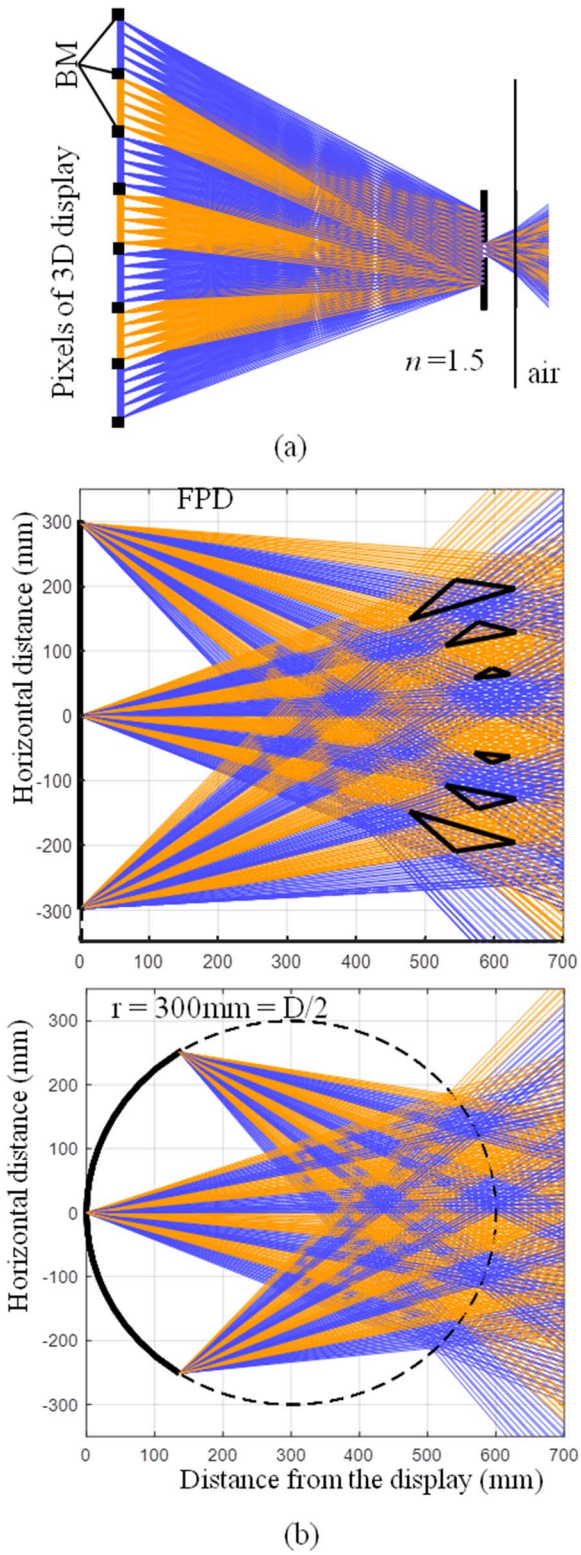

Fig. 8. (a) Trajectories of multiple rays coming from the active area of pixels of the autostereoscopic display through the parallax barrier. BM represented the Black Matrix surrounding the active area of each pixel and width of BM was selected to be 20% of the pixel size. (b) Calculated trajectories of multiple rays coming from the active area of pixels at the three positions on the display for the viewing distance D of 600 mm for the flat surface and curved surface of radius r of 300 mm. Barrier aperture ratio was 15%. Triangles represent the intersection of the calculated trajectories of chief rays from the center, the left edge and the right edge of the display.

each eye. If one eye was located at the areas that these two colored lines were together, this eye would see the pixels assigned for the other eye and the separation of the images for the left

and right eyes were incomplete. Compared with the result of Fig. 5(a) where only 3 chief rays were used, the areas that these two colored lines were together were located around the triangle defined by 3 chief rays coming from the pixel boundaries. And lines of the same colors were located in the viewing zones of Fig. 5(a).

Trajectories by 3 chief rays from the left edge, the center and the right edge of the display defined the viewing zone of autostereoscopic for the ideal case and the triangles by these 3 chief rays represented the area where the separation for the images for the left and the right eyes were not complete. Even when multiple rays other than chief ray from the active area and the boundaries of the pixels were considered for the practical situation, the result by 3 chief rays were still useful as the indicator as illustrated in the calculated result of Fig. 6, 7 and 8.

In case of autostereoscopic 2 view display using the parallax barrier, the condition that the ratio of the radius R and the designed viewing distance D was 1/2 seemed to provide the viewing zones where the area of incomplete separation was much smaller than that for the flat surface. In stereoscopic vision, objects located on the horopter were perceived to be the same and Panum's fusional area was located around the horopter [17], [18]. A theoretical horopter consisted of a circle where the left and right eyes and fixation point were located. Interestingly, if two eyes of the viewer were located at the viewing distance of D, the curved display with the radius of D/2 was located on this theoretical horopter. The radius of the actual empirical horopter was reported to be larger than the theoretical horopter and be concave only for the viewing distance of a few meters. The selection of the radius of the horizontal concave surface for 2D display was reported to be affected by many factors such as the display size, the viewing distance, the reflection, the barrel distortion of the image, the number of the viewers and the difficulty of the bending [6]–[8]. For example, some recommended the radius to be equal to the viewing distance to keep the same viewing distance. Some recommended the radius larger than the viewing distance to reduce the distortion near the display boundary or in consideration of the surface reflection. Generally one radius was reported to have good and bad effects simultaneously and the optimum radius might be different for the specific application. In selecting the proper radius of the curved autostereoscopic display, optical characteristics unique to autostereoscopic displays should be considered together with those factors reported for 2D display.

V. Conclusion

The positions of the viewing zone and the area of the good image separation for the left and the right of the curved autostereoscopic display were investigated by the calculated trajectories of the rays coming from the pixel boundaries at the left edge, the center and the right edge of of the display surface.

The calculated result showed the position of the viewing zones approximately located around the circle whose radius was half of the designed viewing distance and the position of the viewing zones were slightly affected by the ratio R/D of the display radius R and the designed viewing distance D.

On other hand, sizes of triangles by the intersection of trajectories of 3 chief rays from these 3 positions were strongly dependent on the ratio R/D. These triangular sizes tended to decrease as this ratio changes from the infinite at the flat surface toward the ratio of 1/2. These triangles represented the area that the separation of the images for the left and right eyes was incomplete. And the smaller area of these triangles meant the larger area of the good image separation in viewing zones. The calculated trajectories of other rays other than chief rays coming from the pixels boundaries and inside the active area of the pixel showed that the triangles by the intersection of these 3 chief rays were still useful indicator for practical situation.

References

[1] J. S. Yoo *et al.*, "Highly flexible AM-OLED display with integrated gate driver using amorphous silicon TFT on ultrathin metal foil," *J. Display Technol.*, vol. 6, pp. 565–570, 2010.

[2] J. E. Lee *et al.*, "Flexible display driven by solution-processes OTFTs manufactured using All-sputtered electrodes," in *SID Symp. Dig. Tech. Papers*, 2013, vol. 44, pp. 38–40.

[3] D. Hertel, "Viewing direction measurements on flat and curved flexible E-paper displays," *J. Soc. Inf. Display*, vol. 21, pp. 239–248, 2013.

[4] K. C. Heo, Y. Sohn, J. Ye, J. H. Kwon, and J. S. Gwag, "Flexible reflective color displays using thermochromic pigments," *J. Opt. Soc. Korea*, vol. 17, pp. 428–432, 2013.

[5] J. C. Heikenfeld, "Flexing and stretching," *Inf. Information Displays*, vol. 29, pp. 30–34, 2013.

[6] N. S. Roh, "The curved display makes an impression," *Inf. Display*, vol. 30, no. 6, pp. 34–39, 2014.

[7] H. K. Hong, "Analysis of the reflected image by the cylindrical concave surface of the mobile display," *J. Soc. Inf. Display*, vol. 22, pp. 163–169, 2014.

[8] Y. Park, J. J. Yoo, D. Kang, and S. Kim, "Quantification model of proper curvature for large-sized curved TVs," *J. Soc. Inf. Display*, vol. 23, no. 3, pp. 391–396, 2015.

[9] B. Javidi and F. Okano, *Three–Dimensional Television, Video, and Display Technologies Berlin*. Germany: Springer, 2002.

[10] J. Y. Son and B. Javidi, "Three-dimensional imaging method based on multiview images," *J. Display Technol.*, vol. 1, no. 1, pp. 125–140, Sep. 2005.

[11] H. Yamamoto, T. Kimura, S. Matsumoto, and S. Suyama, "Viewing-zone control of light-emitting diode panel for stereoscopic display and multiple viewing distances," *J. Display Technol.*, vol. 6, no. 9, pp. 359–366, Sep. 2010.

[12] H. K. Hong and M. J. Lim, "Determination of luminance distribution of autostereoscopic 3-D displays through calculation of angular profile," *J. Soc. Inf. Display*, vol. 18, pp. 327–335, 2010.

[13] C. H. Lee, J. Y. Son, S. K. Kim, and M. C. Park, "Visualization of viewing zones formed in a contact-type multiview 3D imaging system," *J. Display Technol.*, vol. 8, no. 9, pp. 546–551, Sep. 2012.

[14] W. H. Hsu *et al.*, "A study of optimal viewing distance in an AS3D display," in *SID Symp. Dig. Tech. Papers*, 2013, vol. 44, pp. 1198–1201.

[15] H. K. Hong, "Design of autostereoscopic two-view 3D that use the spherical concave surface and parallax barrier," *J. Soc. Inf. Display*, vol. 22, pp. 144–152, 2014.

[16] Matlab [Online]. Available: www.mathwork.com, Feb. 2014

[17] R. Patterson, "Review paper: Human factors of stereo displays: An update," *J. Soc. Inf. Display*, vol. 17, pp. 987–996, 2009.

[18] I. P. Howard and B. J. Rogers, *Perceiving in Depth*. New York, NY, USA: Oxford Univ., 2012, vol. 2, Stereoscopic Vision.

Hyung Ki Hong received the B.S. degree from Seoul National University and the Ph.D. degree from Korea Institute of Science and Technology (KAIST), both in physics.

After receiving the Ph.D. degree in 1998, he joined LG Display (formerly LCD division of LG Electronics) and worked for the performance improvement and the performance characterization of LCD and 3D display until 2010. His main interest is the human factors related to the display and 3D display. He works as IEC members for the standardization of 3D display performance. He has been an Associate Professor with the Department of Optometry, Seoul National University of Science and Technology, since 2010.